

### ABSTRACT

The combined and synergistic effects of clay colloids and pore water velocity on virus transport and retention in porous media were examined at three pore water velocities (0.38, 0.74, and 1.21 cm/min). The results indicated that the mass recovery of viruses and clay colloids decreased as the pore water velocity decreased; whereas, for the cotransport experiments no clear trend was observed. Mass recovery values for both viruses, calculated based on total virus concentration in the effluent, were reduced compared to those in the absence of clays. The transport of both suspended and attached onto suspended clay-particles viruses was retarded, compared to the tracer, only at the highest pore water velocity. Moreover both clay colloids were shown to hinder virus transport at the highest pore water velocity. At the lower velocities MS2 transport was hindered and  $\Phi$ X174 transport was facilitated with the exception of  $U=0.74$  cm/min in the presence of KGa-1b. Both MS2 and  $\Phi$ X174 were attached in greater amounts onto KGa-1b than STx-1b. Also, MS2 exhibited greater affinity than  $\Phi$ X174 for both clays.

### MATERIALS

#### Bacteriophages

**MS2:** an F-specific single-stranded RNA phage with effective particle diameter ranging from 24 to 26 nm

**$\Phi$ X174:** a somatic single-stranded DNA phage with effective particle diameter ranging from 25 to 27 nm

#### Clays

**Kaolinite (KGa-1b):** a well-crystallized kaolin from Washington County, Georgia  
**Montmorillonite (STx-1b):** a Ca-rich montmorillonite, white, from Gonzales County, Texas

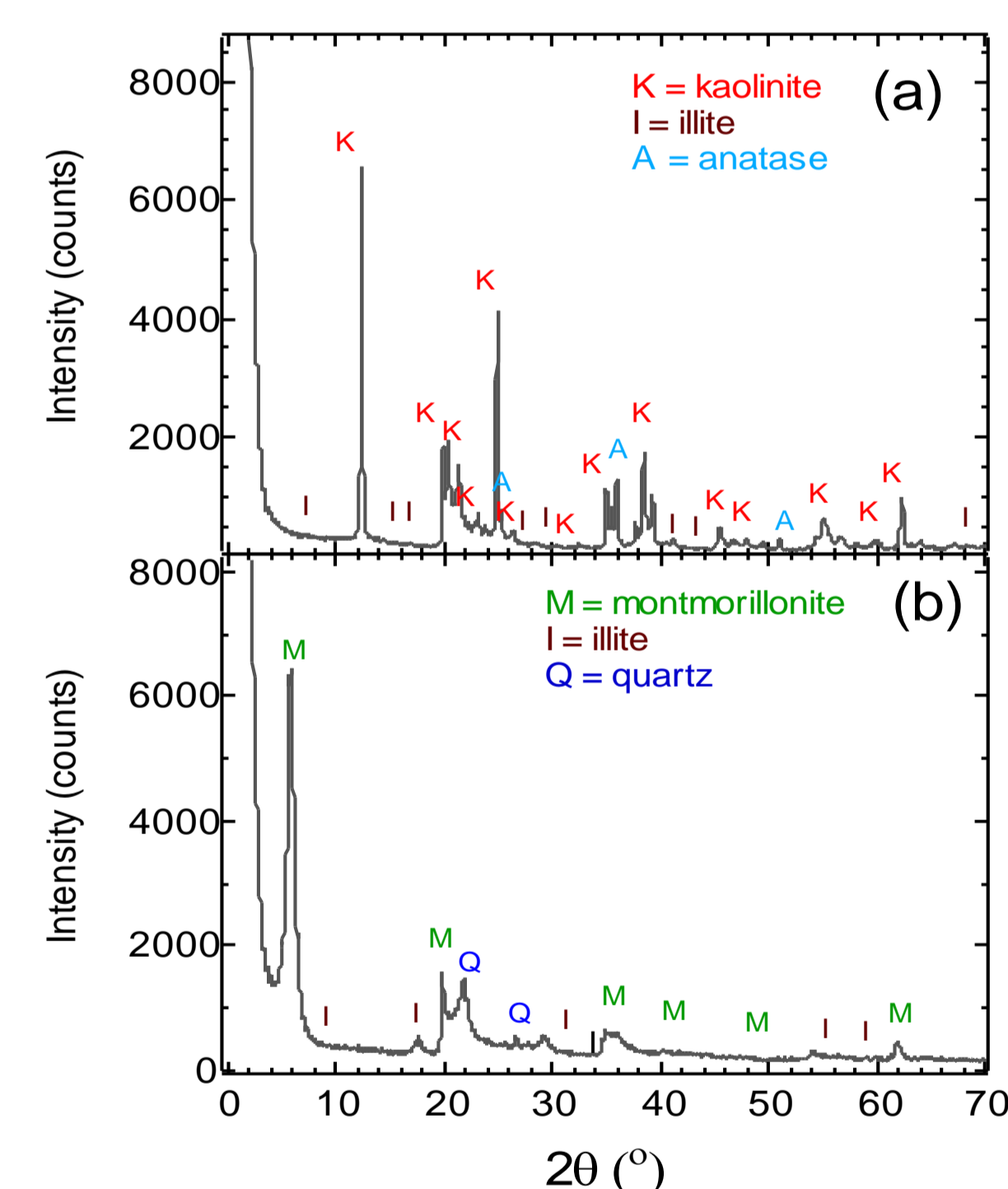


Figure 1. X-ray diffraction patterns of (a) KGa-1b, and (b) STx-1b.

The <2  $\mu$ m clay colloidal fraction was separated by sedimentation and then was purified (Rong et al., 2008). The optical density of the clay colloids was analyzed at a wavelength of 280 nm by a UV-vis spectrophotometer. Using calibration curves, each measured KGa-1b absorbance was converted to KGa-1b concentration and each measured STx-1b absorbance was converted to STx-1b concentration.

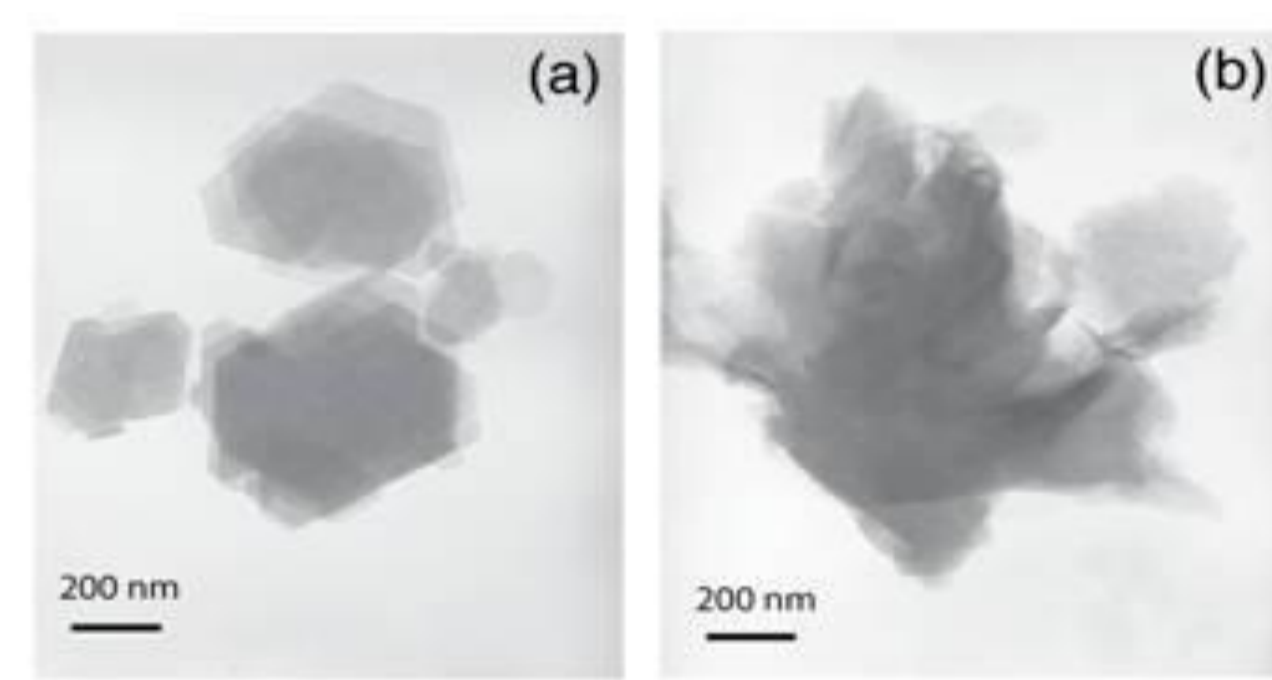


Figure 2. Transmission electron micrographs of (a) KGa-1b, and (b) STx-1b.

### METHODS

#### Column Experiments

- columns (2.5 cm diameter and 30 cm length)
- glass beads 2mm in diameter
- $q=2.5, 1.5$  and  $0.8$  mL/min
- $U=q/\theta=1.21, 0.74,$  and  $0.38$  cm/min
- 3 pore volumes of feed suspension in ddH<sub>2</sub>O
- 5 pore volumes of ddH<sub>2</sub>O solution

#### Cotransport Experiments

- $C_c$ : Suspended clay particles
- $C_{Total-v}$ : Total viruses  $C_{Total-v} = C_v + C_{vc}$
- $C_v$ : Suspended viruses
- $C_{vc}$ : Viruses attached onto suspended clays
- $C_{c^*}$ : Clays attached onto glass beads
- $C_{v^*}$ : Viruses attached onto glass beads
- $C_{vc^*}$ : Viruses attached onto attached clays

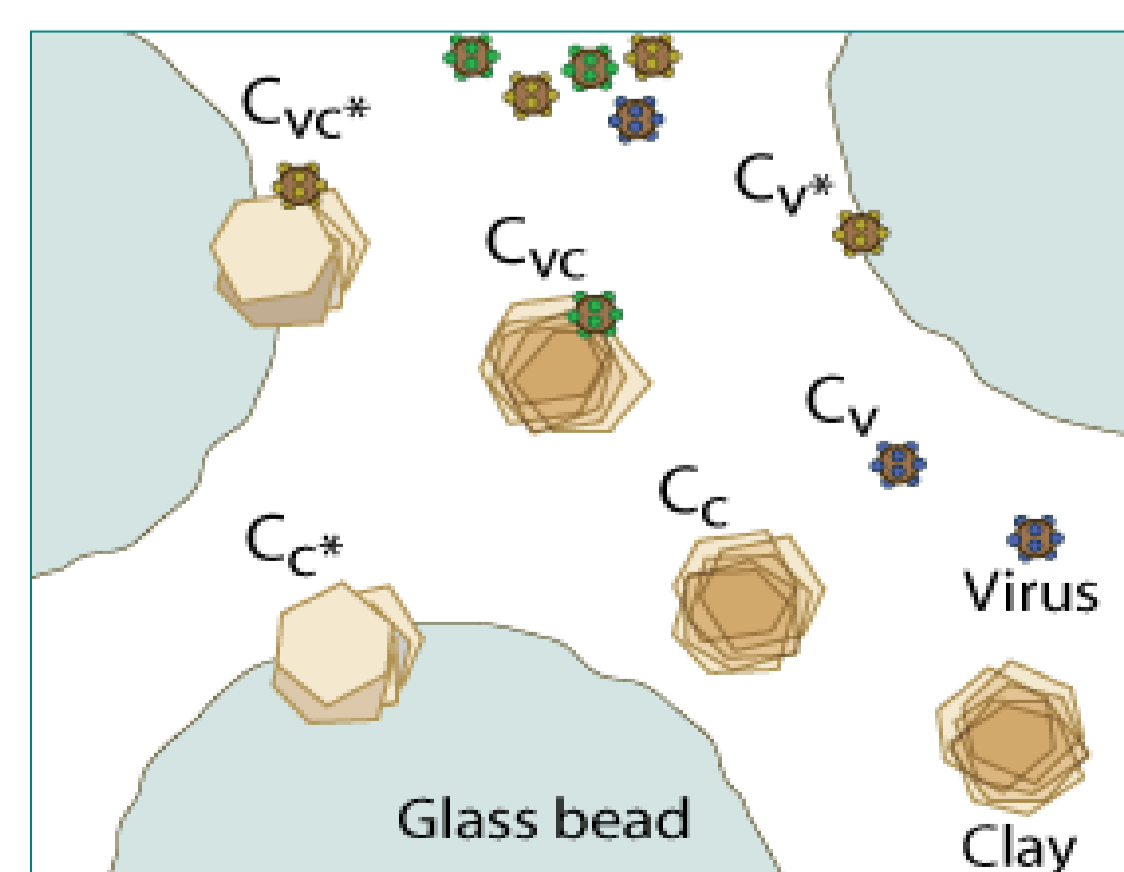


Figure 3. Schematic illustration of the six concentration components involved in cotransport experiments (Syngouna and Chrysikopoulos, 2012).

### THEORY

#### 1. Colloid filtration theory

The dimensionless collision efficiency,  $\alpha$  (Rajagopalan and Tien 1976):

$$\alpha = \frac{2d_c \ln(RB)}{3(1-\theta)\eta_0 L} \quad RB = \frac{M_{r(i)}}{M_{r(0)}} \quad M_r(L) = \int_0^L C_i(L,t) dt$$

The single collector contact efficiency,  $\eta_0$  (Tufenkji and Elimelech, 2004):

$$\eta_0 = 2.4A_s^{1/3} N_R^{-0.081} N_{Pe}^{-0.715} N_{vdW}^{0.052} + 0.55A_s N_R^{1.675} N_A^{0.125} + 0.22N_R^{-0.24} N_G^{1.11} N_{vdW}^{0.053}$$

#### 2. Moment Analysis

$$M_n(x) = \frac{\int_0^x t^n C_i(x,t) dt}{\int_0^\infty C_i(x,t) dt}$$

#### 3. Virus-glass and clay-glass beads interactions

##### a. Classical DLVO theory (Loveland et al., 1996)

$$\Phi_{DLVO}(h) = \Phi_{vdW}(h) + \Phi_{dl}(h) + \Phi_{Bom}(h)$$

##### b. Extended DLVO theory (Bergendahl and Grasso, 1999)

$$\Phi_{XDLVO}(h) = \Phi_{DLVO}(h) + \Phi_{AB}(h)$$

### RESULTS

#### Transport Experiments

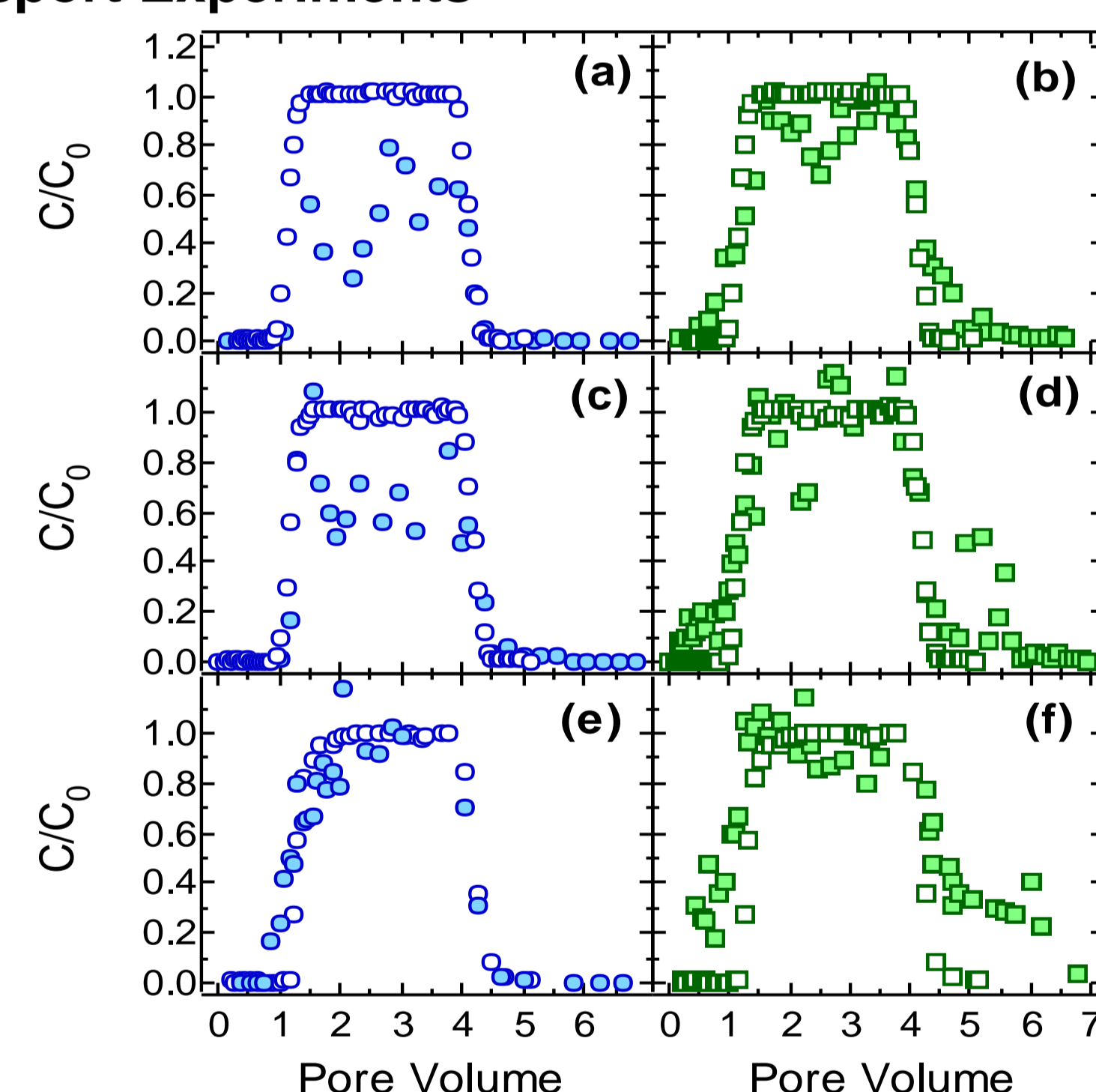


Figure 4. Experimental data for transport of chloride tracer (open symbols), bacteriophages MS2 (filled circles), and  $\Phi$ X174 (filled squares) with  $U$  equal to: (a,b) 0.38, (c,d) 0.74, and (e,f) 1.21 cm/min.

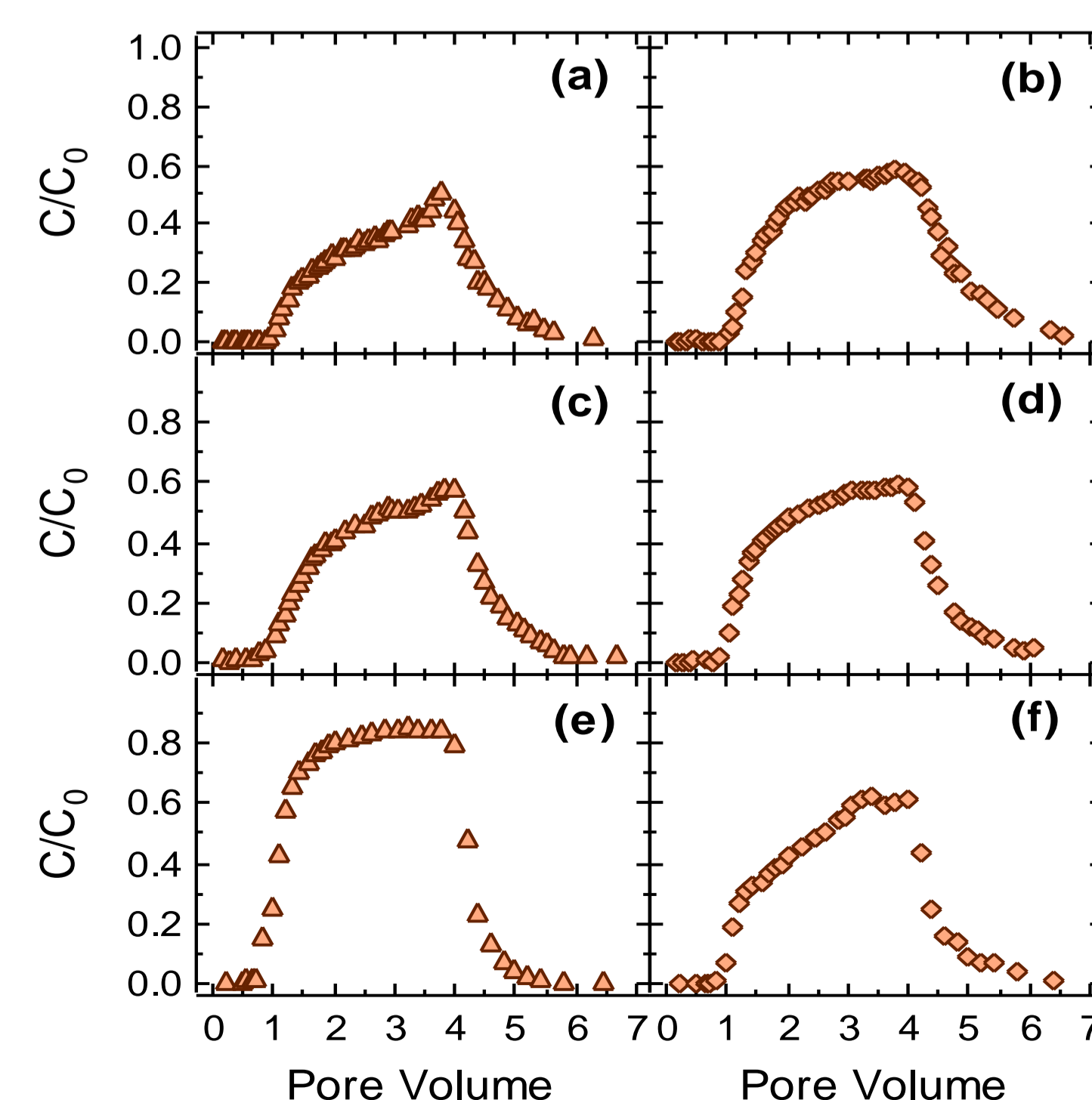


Figure 5. Experimental data (symbols) for transport of KGa-1b (triangles), and STx-1b colloids (diamonds) with  $U$  equal to: (a,b) 0.38, (c,d) 0.74, and (e,f) 1.21 cm/min.

#### Cotransport Experiments

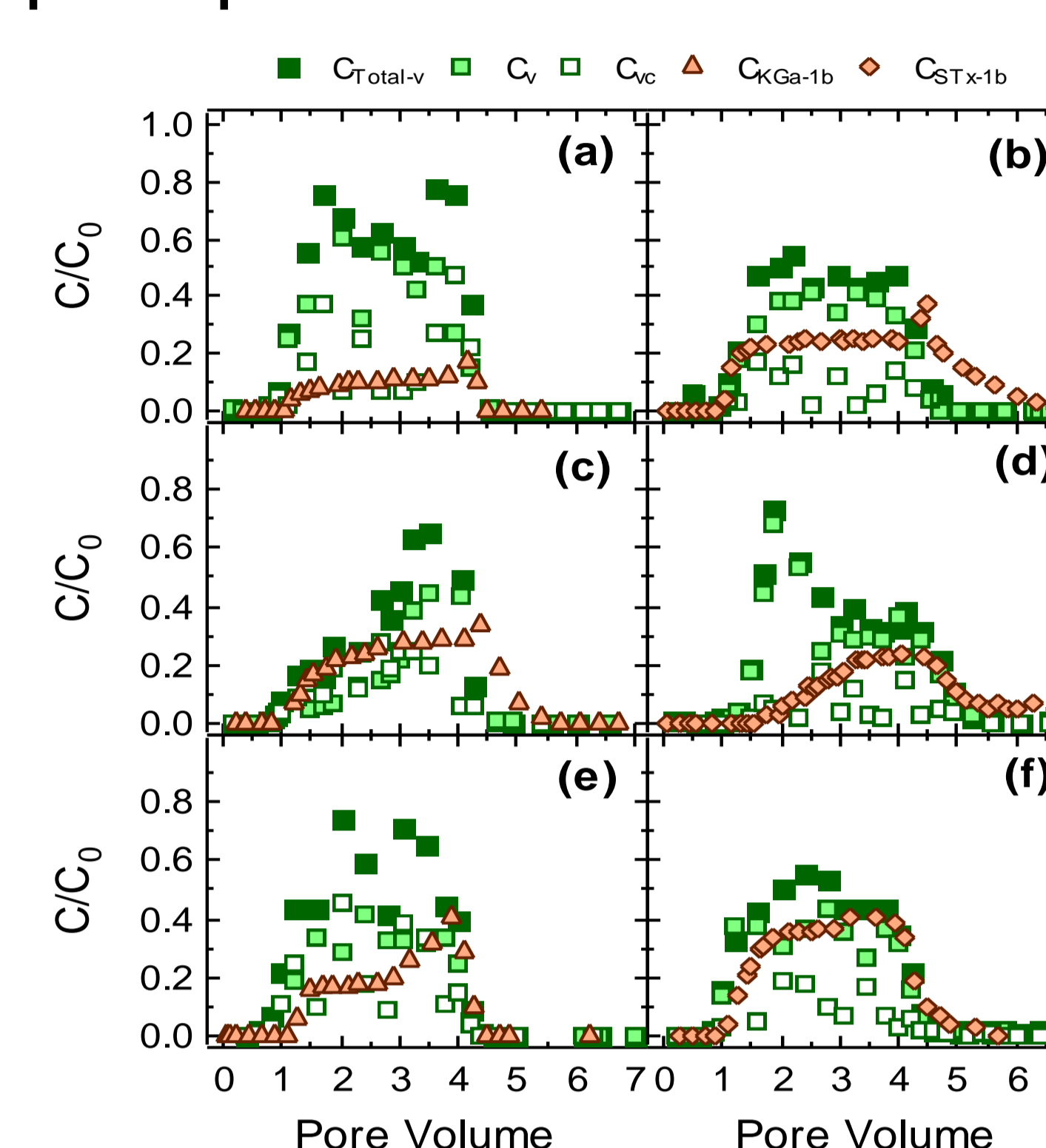


Figure 6. Experimental data for cotransport of  $\Phi$ X174 with KGa-1b (a,c,e), and STx-1b (b,d,f) with  $U$  equal to: (a,b) 0.38, (c,d) 0.74, and (e,f) 1.21 cm/min.

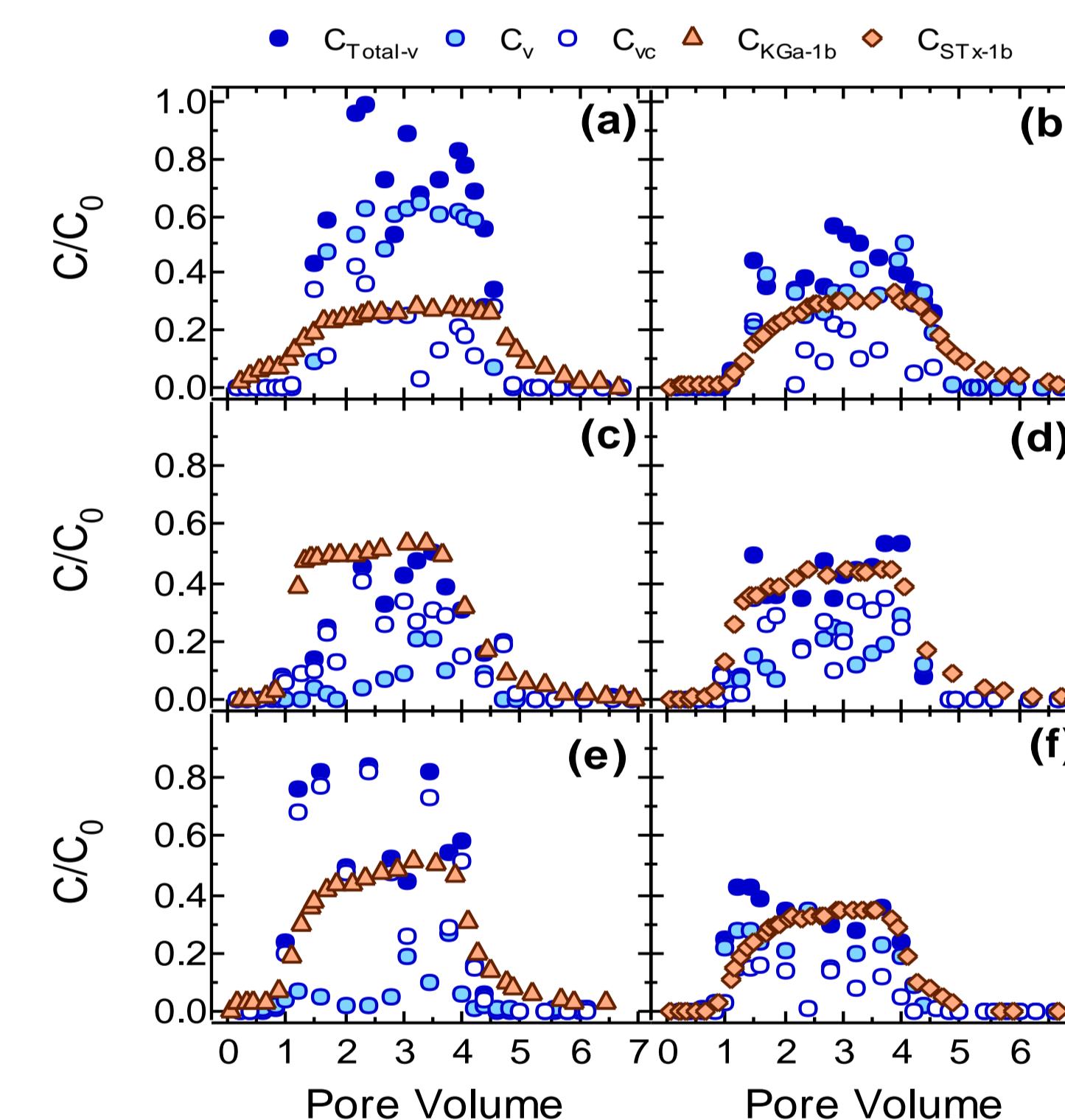


Figure 7. Experimental data for cotransport of MS2 with KGa-1b (a,c,e), and STx-1b (b,d,f) with  $U$  equal to: (a,b) 0.38, (c,d) 0.74, and (e,f) 1.21 cm/min.

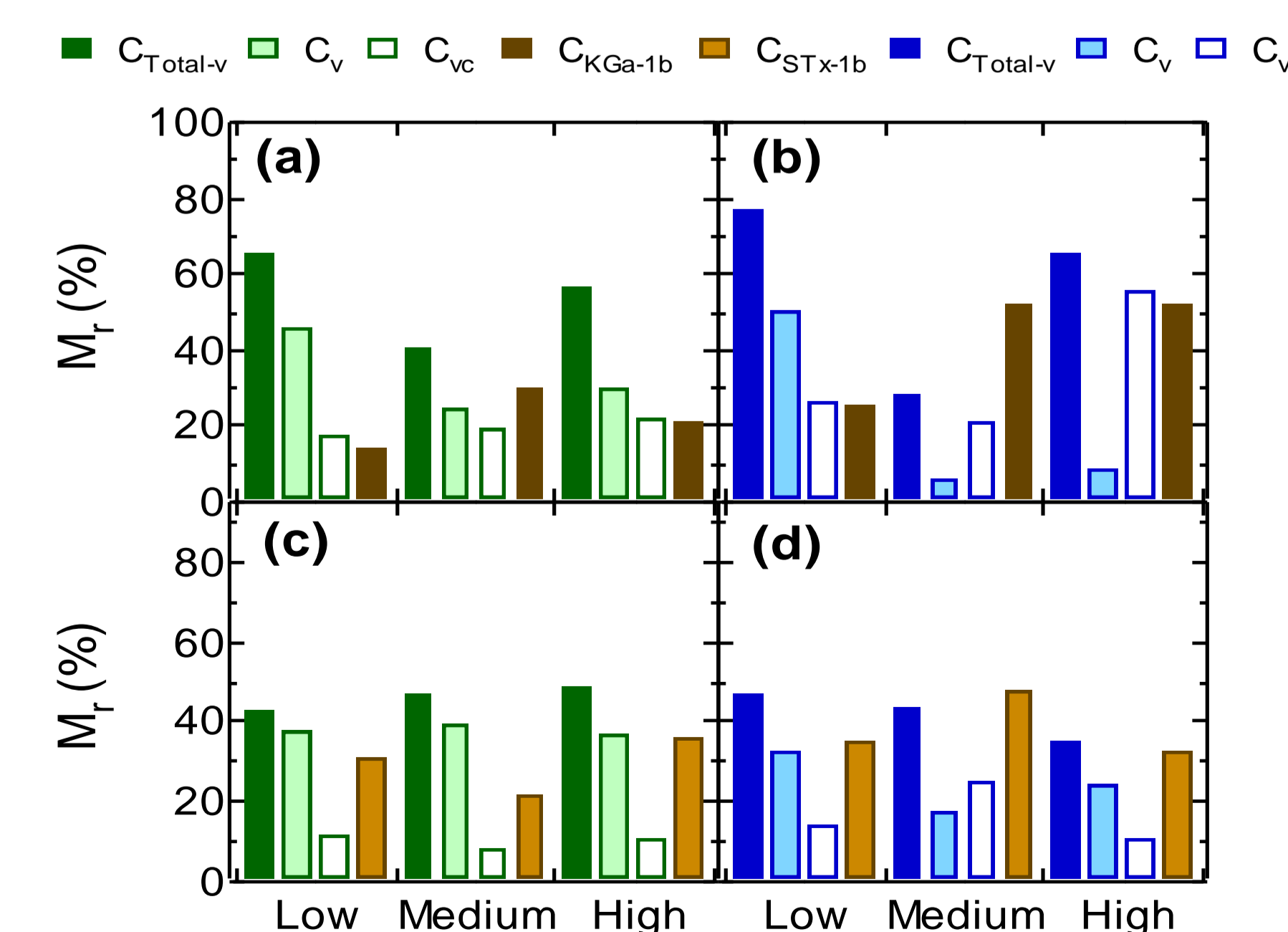


Figure 8. Calculated  $M_r$  values based on  $C_{Total-v}$ ,  $C_v$ ,  $C_{vc}$ , and  $C_c$  for cotransport of: (a)  $\Phi$ X174 with KGa-1b, (b) MS2 with KGa-1b, (c)  $\Phi$ X174 with STx-1b, and (d) MS2 with STx-1b at low ( $U=0.38$  cm/min), medium ( $U=0.74$  cm/min) and high ( $U=1.21$  cm/min) interstitial velocities.

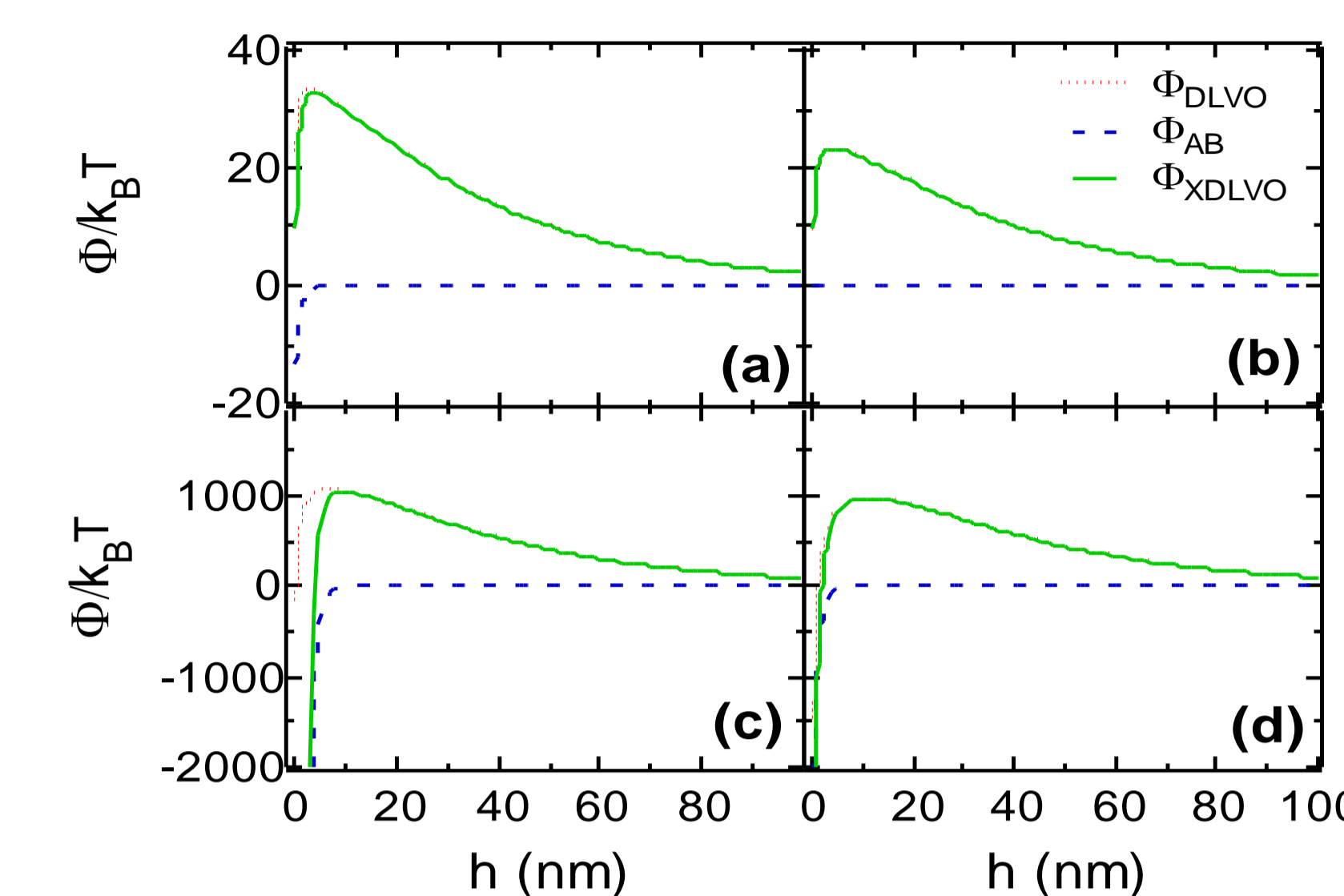


Figure 9. Predicted sphere-plate  $\Phi_{DLVO}$ ,  $\Phi_{AB}$ , and  $\Phi_{XDLVO}$  interaction energy profiles for: (a) MS2 and glass beads, (b)  $\Phi$ X174 and glass beads, (c) KGa-1b and glass beads, and (d) STx-1b and glass beads, as a function of separation distance (here  $pH=7$ ,  $I_s=10^{-4}$  M).

### CONCLUSIONS

#### Transport Experiments

- The peak-concentrations and mass recoveries for both viruses increased with increasing  $U$ .
- With no exception, all estimated  $M_r$  values for MS2 were lower than those of  $\Phi$ X174.
- For the case of the lowest  $U$ , slight enhancement was observed ( $M_{r(i)}/M_{r(0)} > 1$ ) for both viruses.
- Higher mass recoveries observed for STx-1b than KGa-1b for the lowest  $U$ .
- The  $\alpha_{Total-v}$  values of MS2 in the transport experiments were higher than those of  $\Phi$ X174.

#### Cotransport Experiments

- The transport of  $C_{Total-v}$  and  $C_{vc}$  for  $\Phi$ X174 was retarded only at the highest  $U$  compared to the tracer.
- The same trend was observed at the highest  $U$  for  $C_v$  and  $C_{vc}$  of MS2, except KGa-1b presence.
- In most cases, in the presence of KGa-1b,  $C_{vc}$  of  $\Phi$ X174 was enhanced more than  $C_{Total-v}$  of  $\Phi$ X174.
- For all cases examined,  $C_v$  of MS2 was enhanced more than  $C_{Total-v}$  of MS2, and  $C_{Total-v}$  of MS2 was enhanced more than  $C_{vc}$  of MS2 for both clays employed (KGa-1b, STx-1b).
- In the presence of KGa-1b, the  $M_r$  values based on  $C_{vc}$  of MS2 were quite high (21.4 to 55.4%).
- In the presence of STx-1b, the  $M_r$  values based on  $C_{Total-v}$  of MS2 were lower.
- The  $M_r$  values based on  $C_{vc}$  of  $\Phi$ X174 were considerably lower than those of MS2.
- The  $\alpha_{Total-v}$  values were higher for both viruses in all cases examined, which indicated that more attachment sites were available on the solid matrix (glass beads and  $C_c$ ).
- In the presence of STx-1b,  $\alpha_{Total-v}$  values decreased with decreasing  $U$ , while in the presence of KGa-1b no clear trend was observed.

### REFERENCES

- Chrysikopoulos, C. V.; Syngouna, V.I. *Colloids and Surfaces B: Biointerfaces*. 92 (2012) 74-83.
- Syngouna V.I.; Chrysikopoulos, C.V. *Colloids and Surfaces A: Physicochem. Eng. Aspects*. (2012) In press
- Rong, X.; Huang, Q.; He, X.; Chen, H.; Cai, P.; Liang, W. *Colloids and Surfaces B: Biointerfaces*. (2008) 49-55.
- Rajagopalan, R.; Tien, C. *AIChE J.* 22 (1976) 523-533.
- Tufenkji, N.; Elimelech, M. *Environ. Sci. Technol.* 38 (2004) 529-536.
- Loveland, J.P.; Ryan, J.N.; Amy, G.L.; Harvey, R.W. *Colloids Surf. A: Physicochem. Eng. Aspects* 107 (1996) 205-221.
- Bergendahl, J.; Grasso, D. *AIChE J.* 45 (1999) 475-484.

#### ACKNOWLEDGMENTS



This research has been co-financed by the European Union (European Social Fund-ESF) and Greek National Funds through the Operational program "Education and Lifelong Learning" under the action Aristeia I (Code No. 1185)